

AN ADAPTIVE METHOD TO FOCUSING IN AN UNKNOWN SCENARIO

L. Crocco^{1, *}, L. Di Donato², D. A. M. Iero², and T. Isernia²

¹CNR-IREA, National Research Council of Italy-Institute for Electromagnetic Sensing of the Environment, via Diocleziano 328, Naples 80124, Italy

²DIMET — University Mediterranea of Reggio Calabria, via Graziella, loc. Feo di Vito, Reggio Calabria 89060, Italy

Abstract—The problem of field focusing onto a target location in an unknown scenario is considered. In particular, we devise an adaptive procedure in which first an image of the unknown region where the target point is located is formed via the linear sampling method (LSM). Then, the LSM result is used also to define the excitations coefficients for the array elements needed to focus the field. This novel approach to focusing is described and tested with numerical examples.

1. INTRODUCTION

The problem of focusing a time-harmonic wave in an unknown medium is an open problem in wave physics [1, 2], and its solution is relevant from both a theoretical and practical point of view. In fact, it is an extension of the classic electromagnetic focusing problem in which one wants to determine the features of a source capable of radiating a field focused in a given target direction in free space. Moreover, the problem has also a practical relevance, as it is of interest in those applications in which it is necessary to concentrate the energy of a wave into a given region, while taking into account the effects of the unknown (or partially unknown) scenario. In particular, this is indeed the case in several medical treatments, (such as hyperthermia and selective drug delivery) where the “target” point is well known, whereas the scenario is (at most) only approximately known [3–5].

Received 1 May 2012, Accepted 21 June 2012, Scheduled 30 August 2012

* Corresponding author: Lorenzo Crocco (crocco.l@irea.cnr.it).

Typically, the wave to be focused is radiated by an array of probes, and a proper arrangement of their excitations makes it possible to produce the desired field. Hence, the problem can be formulated as a synthesis problem aimed at determining the excitations coefficients of the array elements.

The “standard” focusing problem in free space has been broadly addressed in literature. In particular, an effective way to solve the problem is to cast it as a convex programming (CP) problem [6], as this allows to achieve an optimal solution without the need of computationally intensive global optimization procedures. As long as the scenario is known, CP approaches can be successfully applied also to non-homogeneous scenarios [7, 8]. Conversely, they are not viable when the scenario is unknown, as they require the exact knowledge of the field in the target region due to each antenna.

Accordingly, the problem we are considering here is usually tackled in an *adaptive* way, that is splitting the focusing task into two parts: a *sensing* stage meant at gaining some information on the unknown environment and the actual *focusing* of the field, which consists in determining the excitation coefficients taking into account the acquired knowledge. For instance, the method proposed by Haddadin and Ebbini to focus acoustic waves [9] moves in this direction, as it aims to tackle an inverse scattering problem [10] to achieve information on the medium at hand by processing the field it backscatters during the sensing stage. The estimated scenario is then used to cast a “standard” focusing problem. However, inverse scattering problems are non-linear and ill-posed, so that significant errors or uncertainties may result from the sensing stage processing. In addition, inverse scattering procedures are computational expensive, thus affecting the overall efficiency of such an approach.

A more effective and widely adopted procedure is the time reversal mirror introduced by Fink [11], which has been applied to a variety of focusing problems involving acoustic or electromagnetic waves. In particular, the method consists in exploiting the measured data (after a phase conjugation) to supply the excitations that concentrate the energy on the “strongest” scatterer. Iterating the measure-reverse process allows to improve the energy localization. However, the method does not allow to select the target point at will, unless the scenario is known, which is obviously not the case at hand.

In this paper, we propose a novel adaptive focusing strategy based on the linear sampling method (LSM) [12, 13].

The LSM is one of the most popular and effective approaches to image the morphology of an object from a simple processing of the field it scatters. The method requires the solution of a linear

inverse problem to get an estimate of the target's shape and does not involve approximations. As such, it allows to tackle, within a linear framework, the non-linearity arising from multiple interactions that characterize the wave scattering phenomenon. On the other hand, a recently proposed interpretation of the physics underlying LSM [14] has suggested interesting relationships with the problem of focusing the electromagnetic field in presence of an obstacle.

Hence, we herein propose an adaptive two-steps procedure in which the *sensing* stage consists in imaging the region of interest via LSM processing, while the *focusing* stage is a straightforward exploitation of the LSM solution to determine the excitation coefficients needed to focus the field in the target point. In the following, this strategy, which can be exploited within the range of applicability of the LSM, will be described and tested with respect to canonical 2D scalar electromagnetic problems. A comparison with a focusing procedure based on the incident field in the reference background, i.e., neglecting the presence and the nature of the anomalies, is also provided.

The paper is organized as follows. In Section 2, the LSM basics are briefly revised. In Section 3, the proposed focusing procedure is described. The method's implementation and a numerical assessment are then given in Section 4, followed by conclusions. Throughout the paper the time harmonic factor $\exp\{j\omega t\}$ is assumed and omitted.

2. THE LINEAR SAMPLING METHOD: A REVIEW

In the following, the basics of the LSM are reviewed with respect to the canonical 2-D scalar electromagnetic scattering problem. To this end, let us suppose that an unknown (possibly not connected) scatterer, whose cross section Σ is invariant along the z -axis, is hosted in a region under test Ω and it is probed by means of transmitting and receiving antennas polarized along the target's axis of invariance, which lie on a closed curve Γ^\dagger .

Let us denote as $I_p(\theta)$ the (known) excitations of the array elements located on Γ in the direction θ and with $E_{\text{inc}}(\underline{r}, \theta)$ the *incident* wave it radiates in Ω at a fixed frequency when no target is present. Finally, $E_s(\underline{R}, \theta)$ denotes the corresponding scattered far-field as measured on $\underline{R} \in \Gamma$.

To estimate the shape Σ , the LSM requires to sample Ω into an arbitrary grid of sampling points \underline{r}_p and solve, in each of them, the so

[†] Without loss of generality we assume that Γ is a circumference.

called “far field integral equation” (FFIE):

$$\mathcal{F}[x] = \int_{\Gamma} E_s(\underline{R}, \theta) x(\theta, \underline{r}_p) d\theta = G(\underline{R}, \underline{r}_p), \quad (1)$$

wherein x is the unknown function, the right-hand side G expresses the background Green’s function for the considered sampling point (that is the field radiated on $\underline{R} \in \Gamma$ by an elementary source located in \underline{r}_p , when the targets are not present) and \mathcal{F} synthetically denotes the “far-field” operator defined through the left hand side of the FFIE [12].

The solution of (1) for all the sampling points in Ω allows to estimate the unknown shape. As a matter of fact, the L^2 -norm (i.e., the “energy”) of the unknown function $x(\theta, \underline{r}_p)$, i.e.,

$$\Upsilon(\underline{r}_p) = \left[\int_{\Gamma} |x(\theta, \underline{r}_p)|^2 d\theta \right]^{1/2}, \quad (2)$$

depends on the sampling point as it becomes unbounded when $\underline{r}_p \notin \Sigma$, and keeps bounded elsewhere. As such, Υ plays the role of a support indicator, as its plot over the region under test Ω directly provides an image of the target’s shape [12, 13].

Due to the compactness of \mathcal{F} , the problem cast through the FFIE is ill-posed and has to be solved in regularized fashion. Accordingly, for each sampling point the unknown function x is determined as:

$$x = x_{\text{ME}} : \arg \min \{ \|\mathcal{F}[x] - G(\underline{R}, \underline{r}_p)\|^2 + \alpha \|x\|^2 \}, \quad (3)$$

wherein α is the weighting parameter of the adopted Tikhonov regularization method. The explicit expression of such a *minimum energy* solution x_{ME} , and therefore of the LSM indicator Υ , can be actually achieved by evaluating the singular value decomposition (SVD) of \mathcal{F} and by computing the solution in each sampling point. For further details on the theoretical background and on the implementation, the reader is referred to [13] and [14, 15], respectively.

3. ADAPTIVE FOCUSING VIA LSM

The physical interpretation given in [14] suggests that the inverse problem cast through the FFIE (1) can be regarded as an attempt to focus in a neighborhood of the sampling point at hand the volumetric current induced by the interaction between a suitable probing wave and the target [14, 16].

To recall this concept, and to show its usefulness in the framework we are considering, let us start observing that the left hand side of (1) expresses a scattered field, say E_s^{LSM} , as it results from the linear

combination, according to $x(\theta, \underline{r}_p)$, of the scattered fields actually measured when probing the unknown scenario with the incident waves radiated by the array antennas, E_{inc} . Owing to the linear relationship which holds between incident fields and scattered ones, it follows that, as long as Equation (3) is fulfilled, the expression:

$$E_{inc}^{LSM}(\underline{r}, \underline{r}_p) = \int_{\Gamma} x(\theta, \underline{r}_p) E_{inc}(\underline{r}, \theta) d\theta, \quad (4)$$

defines an incident wave that, interacting with the target, gives raise to the scattered field E_s^{LSM} on Γ .

Similarly, recalling that incident fields and antennas excitations are linearly related, the source

$$I_p^{LSM}(\theta, \underline{r}_p) = x(\theta, \underline{r}_p) I_p(\theta), \quad (5)$$

identifies the probes excitations distribution required to radiate the field E_{inc}^{LSM} by means of the array antennas at hand. Hence, the solution of the FFIE provides a direct information on the array excitations required to enforce on Γ the scattered field E_s^{LSM} .

According to the LSM formulation, the scattered field arising from the FFIE for a sampling point \underline{r}_p belonging to the target matches in the L^2 norm the field $G(\underline{R}, \underline{r}_p)$ radiated by an elementary source embedded in the reference scenario and located in the target point \underline{r}_p . Hence, as long as $\underline{r}_p \in \Sigma$, the FFIE's solution in \underline{r}_p provides the array excitations required to enforce the scattered field $G(\underline{R}, \underline{r}_p)$ on Γ . It is worth to remark that, as the LSM solution is achieved through a regularized inversion, such a coefficients distribution is a minimum energy one, which therefore excludes super-directive sources [17] and obeys to physical realizability constraints.

Let us now note that:

- (i) the incident wave E_{inc}^{LSM} , as well as the excitation distribution I_p^{LSM} , implicitly depend on the unknown scenario at hand (through the LSM solution);
- (ii) the scattered field G resulting from the achieved excitation distribution I_p^{LSM} is instead independent of the scenario, and only depends on the position of the sampling point with respect to Γ ;
- (iii) such an "invariant" scattered field is actually radiated on Γ by the volumetric current J_{LSM} , which arises from the interaction among the incident field E_{inc}^{LSM} and the (unknown) scenario. Again due to the linearity, this volumetric current is given by:

$$J_{LSM}(\underline{r}, \underline{r}_p) = \int_{\Gamma} x(\theta, \underline{r}_p) J_{ind}(\underline{r}, \theta) d\theta, \quad (6)$$

wherein $J_{\text{ind}}(\underline{r}, \theta)$ denotes the current induced in the target when the incident field $E_{\text{inc}}(\underline{r}, \theta)$ impinges on it.

From the above observations, it follows that when considering the FFIE as applied to two different scenarios with respect to the *same* target point, two different volumetric sources (say J_{LSM}^A and J_{LSM}^B) will be induced to supply the *same* field[‡]. As well known, any source (induced or impressed) can be split into a radiating term which supports the field (in our case G) and a non-radiating (NR) component that instead produces a field which identically vanishes outside of the support [18]. Since in the case at hand the two sources J_{LSM}^A and J_{LSM}^B radiate the same field G , it then follows that they have to differ only for the NR component.

As far as the radiating component is concerned, the discussion and the examples in [14] show that, since the field $G(\underline{R}, \underline{r}_p)$ is circularly symmetric around the sampling point \underline{r}_p , it has to be radiated by an induced current whose radiating term is circularly symmetric around \underline{r}_p [§]. In particular, unless peculiar symmetries occur in the scenario [14], this induced current would correspond to an elementary source located in the target point. More precisely, the “invariant” radiating part of J_{LSM} will be a smoothed version of the impulsive current that ideally supports the expected field on Γ , i.e., the field $G(\underline{R}, \underline{r}_p)$. Since such a current will be mostly concentrated in the neighborhood of the target sampling point, it will exhibit the features we would expect when aiming at focusing the wave energy in some target point located in the region under test. As such, this induced current provides a solution for our source synthesis problem.

However, for a given scenario, the actual induced current distribution will also have a NR part which may in principle lead to a completely different spatial distribution with respect to the aforementioned focused one. Hence, it is necessary to gain a better insight on the (scenario dependent) NR part of J_{LSM} .

To this end, let us first recall that in synthesis problems the minimization of the NR part of the synthesized source is an usual aim to pursue, in order to achieve an optimal (or at least sub-optimal) solution. In practice, this is done by enforcing a minimum energy constraint on the problem’s solution, which is then cast as a regularized inverse source problem [10, 19].

More formally, by denoting with \mathcal{A} the linear and compact *radiation* operator that relates the unknown source^{||} to the field, the

[‡] In the least square sense.

[§] This is due to the relationship holding amongst the field and the source, which, being linear, preserves distances and henceforth (circular) symmetry.

^{||} Impressed or, as in our case, induced.

problem to be solved in our case should be cast as

$$\mathcal{A}J = G, \tag{7}$$

whose *minimum energy* solution is obtained through the minimization of the cost functional:

$$\|\mathcal{A}J - G\|^2 + \mu\|J\|^2, \tag{8}$$

that provides a current distribution J which radiates a field that matches (in the least square sense) the desired field G on Γ , while also satisfying the minimum energy constraint expressed through the second term in (8).

With respect to such a problem it is readily noticed that a “solution” built as in (6) will certainly satisfy the first term of the functional (8), thus providing a *generalized solution* of the problem cast through Equation (7) [19]. In fact, J_{LSM} has been indeed constructed in such a way to radiate a field on Γ that matches in the least square sense the field of a point-like source located in the target point.

In addition, among all solutions to (7) that are built as a linear combination of the volumetric sources induced in the unknown target by the incident fields, J_{LSM} also has an interesting energetic property.

In fact, from the Schwartz inequality, it follows that:

$$\|J_{\text{LSM}}(\underline{r}, \underline{r}_p)\|^2 = \left\| \int_{\Gamma} x(\theta, \underline{r}_p) J_{\text{ind}}(\underline{r}, \theta) d\theta \right\|^2 \leq \|J_{\text{ind}}\|^2 \|x\|^2, \tag{9}$$

where

$$\|J_{\text{ind}}\|^2 = \int_{\Omega} \int_{\Gamma} |J_{\text{ind}}(\underline{r}, \theta)|^2 d\theta d\underline{r} \tag{10}$$

is a constant which does not depend on the sampling point. Then, as $x(\cdot, \theta)$ is the minimum energy function fulfilling Equation (1), the right hand side member is the minimum possible upper bound to the energy of currents of kind (6) obeying (7). Therefore, looking for a minimum energy $x(\cdot, \theta)$ function also means to look for a minimum energy induced current J_{LSM} . More precisely, $J_{\text{LSM}}(\underline{r})$ is a minimax solution, i.e., the solution which minimizes the maximum possible value of the energy of the induced currents.

According to the above, we can conclude that the induced current arising in the region under test when illuminated with the incident field radiated by the LSM established source distribution I_p^{LSM} , i.e., (5), will be dominated by its radiating part and hence will be focused in the target point. As such, it provides an answer to the problem we are tackling.

4. METHOD'S IMPLEMENTATION AND NUMERICAL EXAMPLES

By relying on the reasonings given in Section 3, we propose an adaptive focusing procedure articulated into two steps.

- (i) *Sensing stage*: LSM processing of the measured multiview-multistatic scattered fields to characterize the whole domain under test. This provides a map of the energy required to focus any point located in the region under test, and accordingly a map of those locations which belong to the target.
- (ii) *Focusing stage*: selection of the LSM solution pertaining to target point to define the array excitation coefficients. As previously recalled these excitation coefficients are such that super-directivity (i.e., physically unstable behavior) is avoided.

It is worth to note that because of the above interpretation in terms of volumetric currents, the procedure only makes sense when the target point belongs to Σ . Therefore observing the LSM indicator map achieved in the sensing stage allows to appraise for which points the focusing is actually viable or not, thus proceeding with the second stage of the procedure.

The numerical analysis deals with examples wherein a square region Ω with permittivity ε_b embeds the unknown target having arbitrary geometrical and dielectric properties. The investigated region is surrounded by a circular array of antennas adopted both to probe Ω during the *sensing* stage and to simultaneously radiate the fields during the *focusing* stage. The array operates at a fixed working frequency, that is 2 GHz, and it is assumed as embedded into a host medium with permittivity $\varepsilon_b = 10$. For all the examples, the radius of the circular array of antennas is chosen equal to $4.2\lambda_b$, λ_b being the wavelength in the host medium. Moreover, in order to measure the scattered field in a non-redundant way, as well as to provide non super-directive arrays [20], the number of antennas of the array is set to $N \approx 2k_b a$, k_b being the wavenumber in the host medium and a the radius of the minimum circle enclosing the investigated scenario [20, 21].

We have considered the following test beds:

- *Scenario 1*: a square object ($\varepsilon_{\text{obj}} = 12$, $0.5\lambda_b \times 0.5\lambda_b$), Fig. 1(a).
- *Scenario 2*: three identical square objects ($\varepsilon_{\text{obj}} = 25$, $0.5\lambda_b \times 0.5\lambda_b$), Fig. 1(b).
- *Scenario 3*: the same geometry as Scenario 2, but for targets having a larger permittivity ($\varepsilon_{\text{obj}} = 35$), Fig. 1(c).

- *Scenario 4*: a square object ($\varepsilon_{\text{obj}} = 25$, $0.5\lambda_b \times 0.5\lambda_b$), partially surrounded by an high permittivity thin layer (thickness $\delta = 0.1\lambda_b$, $\varepsilon_l = 50$), Fig. 1(d).
- *Scenario 5*: the domain Ω is partially filled by a medium having randomly varying permittivity ($\pm 9\%$, $\varepsilon_{\text{avg}} = 11$) which embeds three square objects ($\varepsilon_{\text{obj}} = 28$, $0.5\lambda_b \times 0.5\lambda_b$), Fig. 1(e).
- *Scenario 6*: a square object ($\varepsilon_{\text{obj}} = 20$, $0.375\lambda_b \times 0.375\lambda_b$), partially surrounded by a thin layer (thickness $\delta = 0.1\lambda_b$, $\varepsilon_l = 30$), enclosed within an high permittivity boundary ($\varepsilon_{\text{bound}} = 70$, $2.25\lambda_b \times 2.25\lambda_b$), Fig. 1(f).

For all the scenarios $N = 34$ (but for the last one where $N = 24$).

First, we have solved the FFIE and computed the LSM indicator Υ in order to appraise where the focusing strategy driven by LSM is actually viable or not (see Fig. 2). In fact, where the indicator Υ assumes low values (with respect to its overall dynamic range), the FFIE admits a solution and thus the method at hand is applicable.

As our original motivation was to compensate for the lack of knowledge (or partial unknowledge) of the scenario, performances of the proposed strategy are also compared with those one can achieve by means of back-propagation technique [22]. In particular, as the initial scenario is supposed to be free space, backpropagation corresponds herein to an (unconstrained) focusing of the incident fields.

A direct comparison of the results achieved by the LSM approach and those based on the focusing of the incident field is obtained by observing the plot of the normalized amplitude of the total electric fields over the scatterer support Σ , (see Figs. 3 and 4). From these plots, one can observe the good performances of the proposed focusing procedure with respect to focusing of the incident field, especially in terms of spatial selectivity. As a matter of fact, the LSM allows to obtain a well focused field while keeping under control the amplitude of the undesired side lobes, which may arise within the scatterer's support. This is in agreement with the underlying physical meaning.

To get a quantitative comparison between the two methods at hand, we introduce the following parameters:

- the *target point deviation (TPD)* — the distance between the target point (marked with a cross in the figures) and the actual location of the field's maximum amplitude;
- the *main lobe size (MLS)* — the size of the field main lobe as calculated at one half of the maximum amplitude;
- the *main lobe eccentricity (MLE)* — main lobe's circularly symmetry expressed as $e = \sqrt{1 - a^2/b^2}$, where a and b represent the main lobe axes;

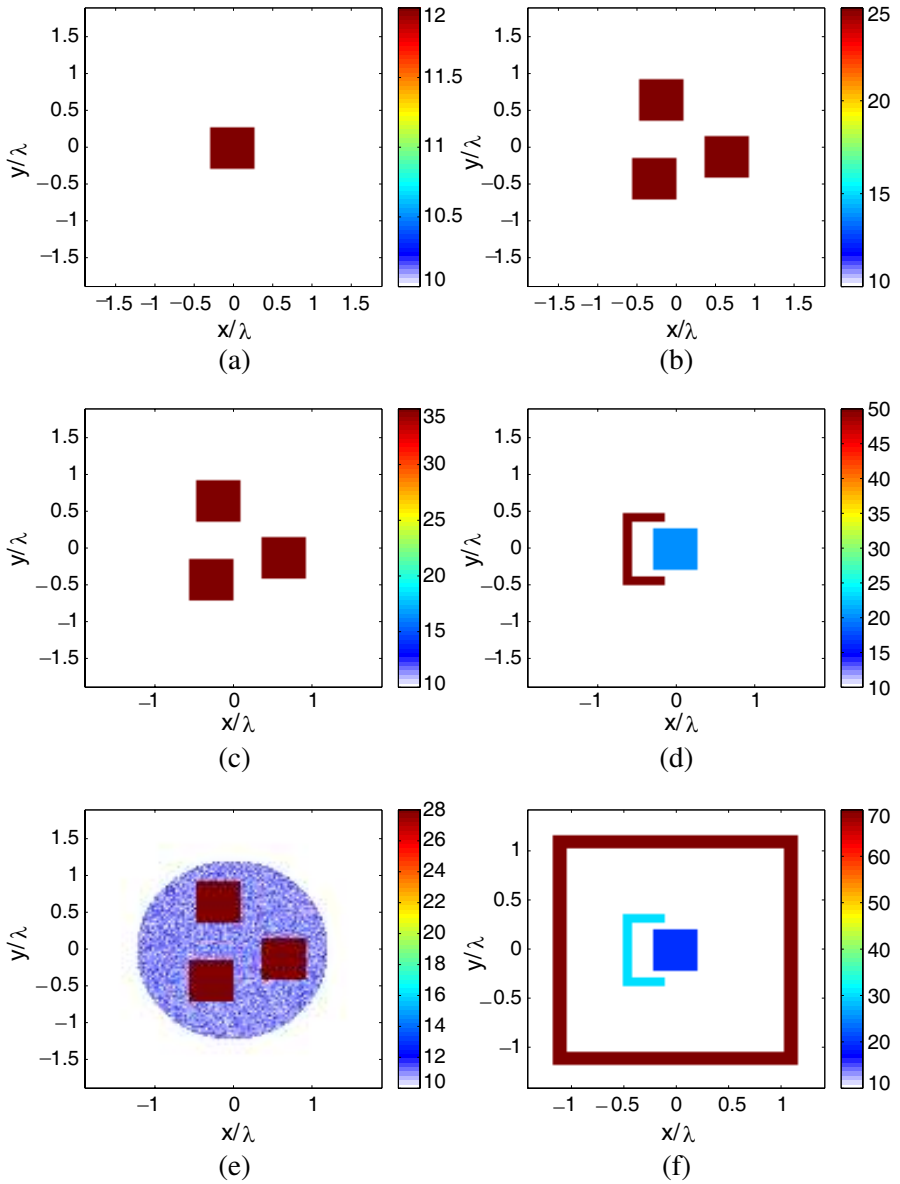


Figure 1. The adopted test beds: (a) Scenario 1; (b) Scenario 2; (c) Scenario 3; (d) Scenario 4; (e) Scenario 5; (f) Scenario 6.

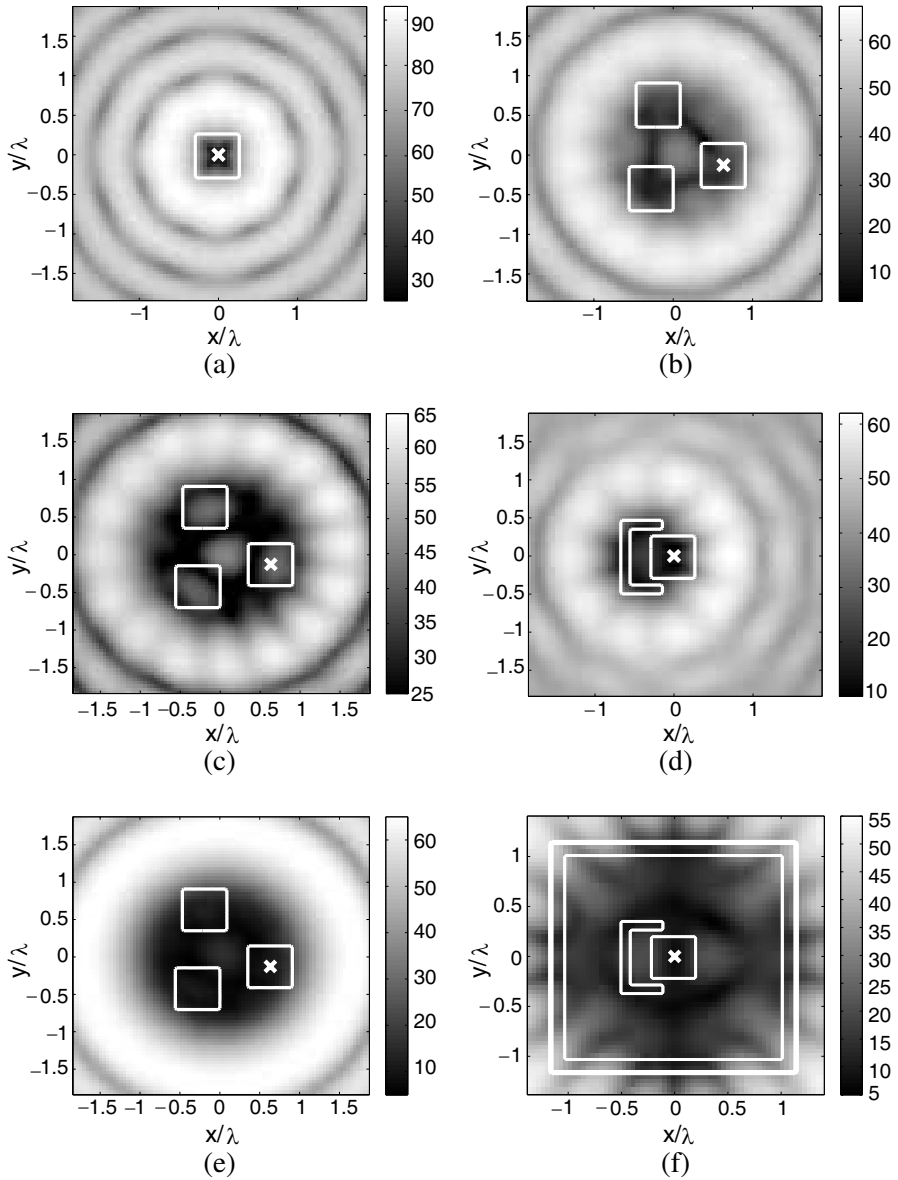


Figure 2. LSM imaging of the considered scenarios: Logarithmic plot of the indicator Υ . Contour plots show actual borders of the targets, while the cross marks the selected focusing target point.

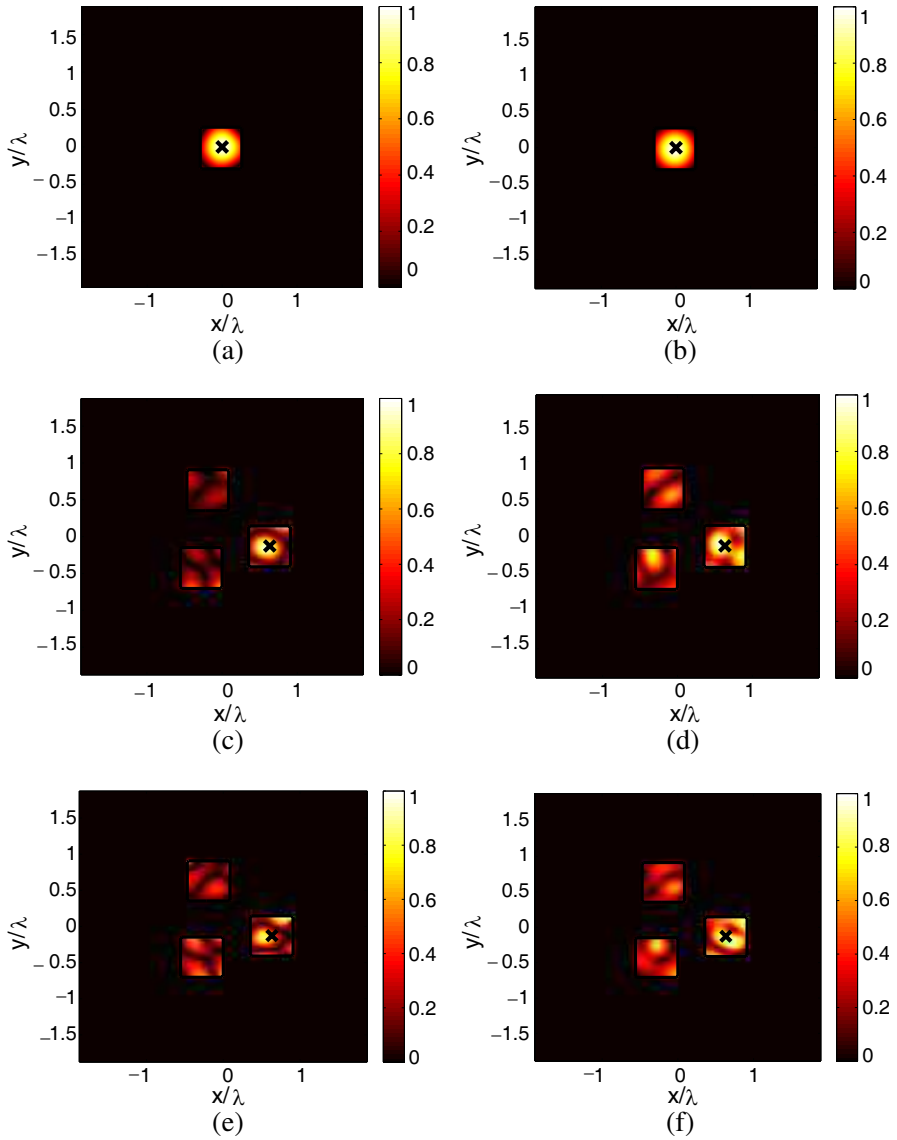


Figure 3. Normalized total field amplitudes over the scatterer support using the synthesized excitations. Left: LSM driven focusing. Right: backpropagation driven focusing. (a), (b) Scenario 1; (c), (d) Scenario 2; (e), (f) Scenario 3.

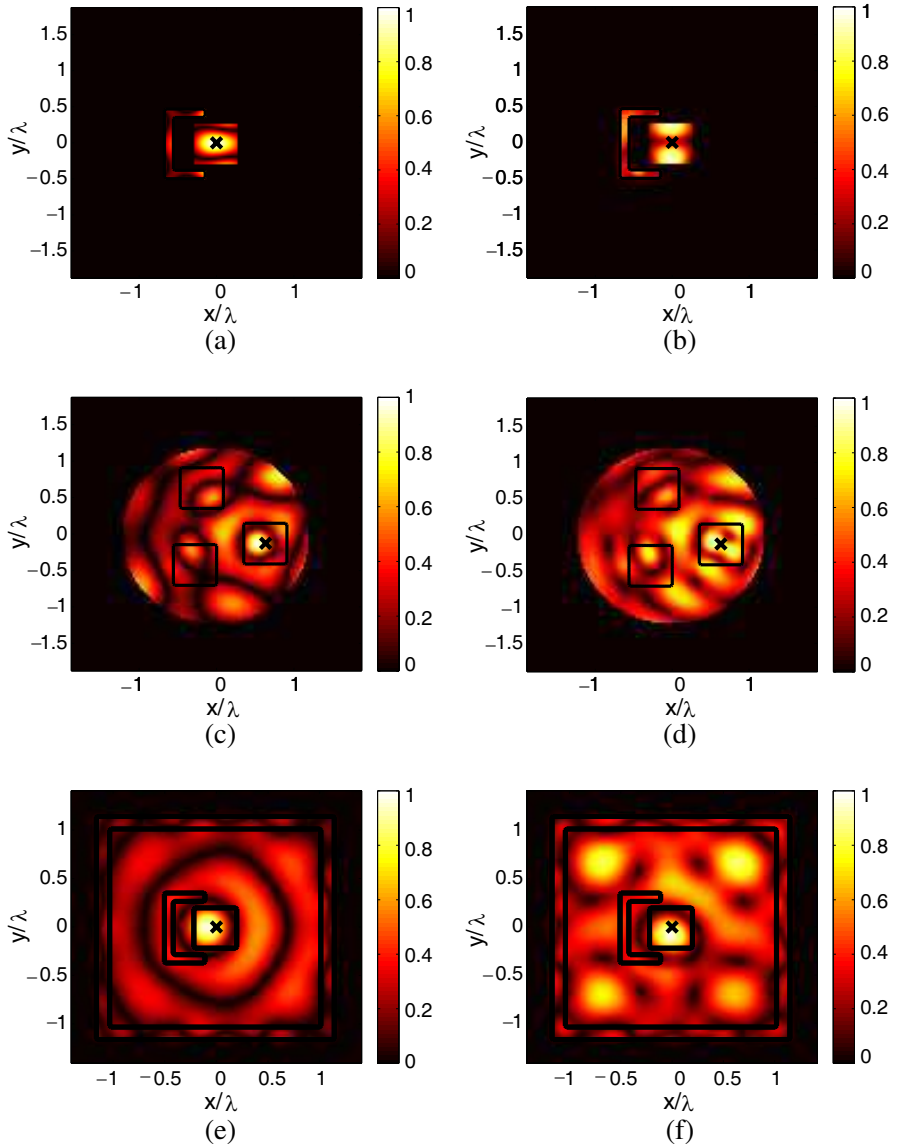


Figure 4. As in Fig. 3, but for scenario (a), (b) 4, (c), (d) 5, and (e), (f) 6.

Table 1. LSM focusing metric parameters.

	TPD [mm]	MLS [mm]	MLE	SLL
Scenario 1	0	10	0.087	-
Scenario 2	3	7.5	0.5	50%
Scenario 3	14.6	10.8	0.92	83%
Scenario 4	0	17.8	0.82	40%
Scenario 5	4.3	13	0	70%
Scenario 6	3	15.5	0.35	60%

Table 2. Backpropagation focusing metric parameters.

	TPD [mm]	MLS [mm]	MLE	SLL
Scenario 1	0	10	0.1	-
Scenario 2	4.2	8.4	0.58	81%
Scenario 3	4.1	13.8	0.82	83%
Scenario 4	8.3	18	0.79	97%
Scenario 5	4.4	31.2	0.91	90%
Scenario 6	3.1	16.6	0.47	85%

- the *side lobes level (SLL)* — amplitude of undesired side lobes surrounding the main one.

The values assumed by these parameters in the different scenarios are summarized in Table 1 and Table 2 for LSM and backpropagation, respectively. As it can be seen, for all cases the proposed LSM based strategy provides results which outperform those obtained by simply focusing the incident fields. This is of course expected, as our method takes multiple interactions into account whereas the incident field neglects them. Such a circumstance also explains why the two approaches have comparable performances in the first test case, where multiple interactions play indeed a minor role. It has also to be noted that performances become worse in case of very strong multiple interactions, see Figs. 3(e) and (f), where the LSM also has lower performances in terms of shape estimation (Fig. 2(c)).

5. CONCLUSION

In this paper, we have presented an approach to the problem of focusing the field radiated by an array of antennas into a target point located

in a bounded region having unknown electromagnetic and morphologic characteristics. This kind of problem is relevant to the case in which the target location is hosted in an inaccessible or unknown region and it has been tackled with an adaptive approach, in which the array probes are first used to image, although qualitatively, the unknown region and then to provide the resulting focused field, and assessed in the case of a $2D$ scalar configuration.

The approach relies on the physical meaning of the LSM, an effective method to tackle the solution of the *inverse obstacle problem*, that is concerned with the imaging of only the shape of unknown scatterers. The method proves to be suitable to our purposes owing to its tight relationship with the problem of focusing a wave in presence of an obstacle. The main features of the approach are related to its effectiveness (only a linear problem has to be solved), as well as to the inherent non approximated nature of the method adopted to *sense* the region under test.

As obvious, limitations of the technique are related to limitations of the LSM, as shown above and in [14]. On the other side, the LSM can be extended in a rather straightforward fashion to the case of Green's functions other than that free space, see for instance [15]. Therefore the proposed focusing approach can be extended to other more cumbersome scenarios as well. In fact an application of the proposed strategy to hyperthermia by exploiting the Green's function of a nominal reference scenario, implying an approximated a priori knowledge of the scenario of interest, is currently being pursued.

ACKNOWLEDGMENT

The authors thank Dr. Ilaria Catapano for useful discussions.

REFERENCES

1. Montaldo, G., M. Tanter, and M. Fink, "Time reversal of speckle noise," *Physical Review Letters*, Vol. 106, No. 5, 054301, 2011.
2. Nabulsia, K. and J. R. Waitb, "Focusing into a lossy medium from an annular slot array," *Journal of Electromagnetic Waves and Applications*, Vol. 7, No. 3, 345–353, 1993.
3. Trujillo-Romero, C. J., S. Garcia-Jimeno, A. Vera, L. Leija, and J. Estelrich, "Using nanoparticles for enhancing the focusing heating effect of an external waveguide applicator for oncology hyperthermia: Evaluation in muscle and tumor phantoms," *Progress In Electromagnetics Research*, Vol. 121, 343–363, 2011.

4. Xiao, S., J. Chen, X. Liu, and B.-Z. Wang, "Spatial focusing characteristics of time reversal UWB pulse transmission with different antenna arrays," *Progress In Electromagnetics Research B*, Vol. 2, 223–232, 2008.
5. Gupta, R. C. and S. P. Singh, "Elliptically bent slotted waveguide conformal focused array for hyperthermia treatment of tumors in curved region of human body," *Progress In Electromagnetics Research*, Vol. 62, 107–125, 2006.
6. Isernia, T. and G. Panariello, "Optimal focusing of scalar fields subject to arbitrary upper bounds," *Electronics Letters*, Vol. 34, 162–164, 1998.
7. Iero, D., T. Isernia, A. F. Morabito, I. Catapano, and L. Crocco, "Optimal constrained field focusing for hyperthermia cancer therapy: A feasibility assessment on realistic phantoms," *Progress In Electromagnetics Research*, Vol. 102, 125–141, 2010.
8. Attardo, E. A., T. Isernia, and G. Vecchi, "Field synthesis in inhomogeneous media: Joint control of polarization, uniformity and SAR in MRI B_1 -field," *Progress In Electromagnetics Research*, Vol. 118, 355–377, 2011.
9. Haddadin, O. S. and E. S. Ebbini, "Ultrasonic focusing through inhomogeneous media by application of the inverse scattering problem," *J. Acoust. Soc. Am.*, Vol. 104, No. 1, 313–325, 1998.
10. Colton, D. and R. Kress, *Inverse Acoustic and Electromagnetic Scattering Theory*, Springer-Verlag, Berlin, Germany, 1992.
11. De Rosny, J., G. Lerosey, and M. Fink, "Theory of electromagnetic time-reversal mirrors," *IEEE Trans. Antennas Propag.*, Vol. 58, No. 10, 3139–3149, 2010.
12. Colton, D., H. Haddad, and M. Piana, "The linear sampling method in inverse electromagnetic scattering theory," *Inverse Probl.*, Vol. 19, 105–137, 2003.
13. Cakoni, F. and D. Colton, *Qualitative Methods in Inverse Scattering Theory*, Springer-Verlag, Berlin, Germany, 2006.
14. Catapano, I., L. Crocco, and T. Isernia, "On simple methods for shape reconstruction of unknown scatterers," *IEEE Trans. Antennas Propag.*, Vol. 55, 1431–1436, 2007.
15. Catapano, I. and L. Crocco, "An imaging method for concealed targets," *IEEE Trans. Geosci. Remote Sens.*, Vol. 47, 1301–1309, 2009.
16. Crocco, L., I. Catapano, L. Di Donato, and T. Isernia, "The linear sampling method as a way to quantitative inverse scattering," *IEEE Trans. Antennas Propag.*, Vol. 60, 1844–1854, 2012.

17. Collin, R. E., *Antennas and Radiowave Propagation*, Electrical Engineering Series, McGraw-Hill International, New York, 1985.
18. Marengo, E. A. and R. W. Ziolkowski, "Nonradiating and minimum energy sources and their fields: Generalized source inversion theory and applications," *IEEE Trans. Antennas Propag.*, Vol. 48, No. 6, 1553–1562, 2000.
19. Bertero, M. and P. Boccacci, *Introduction to Inverse Problems in Imaging*, Institute of Physics, Bristol, UK, 1998.
20. Bucci, O. M. and T. Isernia, "Electromagnetic inverse scattering: Retrievable information and measurement strategies," *Radio Sci.*, Vol. 32, 2123–2138, 1997.
21. Bucci, O. M., C. Gennarelli, and C. Savarese, "Representation of electromagnetic fields over arbitrary surfaces by a finite and non-redundant number of samples," *IEEE Trans. Antennas Propag.*, Vol. 46, 351–359, 1998.
22. Devaney, A. J., "A filtered backpropagation algorithm for diffraction tomography," *Ultrason. Imag.*, Vol. 4, No. 4, 336–350, 1982.